Application of GIS and SWAT Model for Assessing Water Yield at Taguibo River Watershed Forest Reserve (TRWFR), Butuan City, Philippines

Aljon Ente Bocobo[1,2]*, Arnold Gemida Apdohan[1,2], Antonietto Ortega Cacayan Jr.[1], Kenneth John Peña Lajera[2] and Febe Hyacinth Andoy Simbolas[2]

[1]*Department of Agricultural & Biosystems Engineering, College of Engineering and Geosciences, Caraga State University, Ampayon, Butuan City, 8600, Philippines*
[2]*Center for Resource Assessment Analytics and Emerging Technologies (CREATE), Caraga State University, Ampayon, Butuan City, 8600, Philippines*
[3]*Caraga State University,Ampayon, Butuan City, 8600, Philippines*

ABSTRACT

As urban development has progressed, the demand for reliable water supply in Butuan City has increased significantly. However, due to limited water suppliers, the availability of sanitary water could be more inconsistent. Furthermore, the region has experienced heightened occurrences and intensified magnitudes of floods and droughts because of the influence of climate change. Consequently, ensuring an adequate water supply to augment the needs of the growing population has become a pressing concern. Thus, this study developed a hydrological model utilizing the Geographic Information System (GIS) and the Soil and Water Assessment Tool (SWAT) to assess the water yield of the Taguibo River Watershed Forest Reserve. The model was calibrated and validated using monthly average observed discharge data from 2012 to 2013 and 2010 to 2011. The validation phase demonstrated a strong correlation between the model-simulated and actual values, with R^2 = 0.87, NSI = 0.73, and PBIAS= –19%, which revealed the satisfactory performance of the model. These findings underscore the effectiveness of integrating the GIS environment and SWAT model for evaluating watershed hydrology and estimating water yield. Overall, this study showcases the potential of GIS and the SWAT model in comprehensively examining the hydrological aspects of watersheds and providing valuable insights into water yield calculations.

Keywords: Hydrological Model, GIS, SWAT, Taguibo River Watershed Forest Reserve (TRWFR), Water Yield

Aljon Ente Bocobo, Arnold Gemida Apdohan, Antonietto Ortega Cacayan Jr., Kenneth John Peña Lajera and
Febe Hyacinth Andoy Simbolas

INTRODUCTION

Butuan City in the Philippines relies heavily on the Taguibo Watershed for essential ecosystem services, the most significant being its role as a dependable supplier of clean and fresh drinking water to the surrounding communities. In the Caraga Region, this surface catchment also acts as an environmental buffer against harsh or inclement weather (Santillan et al., 2011; Sanguila et al., 2016). Indeed, a reliable water supply is crucial to all living and non-living organisms. According to Kodoatie and Sjarief (2010), water availability refers to the anticipated quantity of water within a designated period existing at a particular site that encompasses various water bodies such as rivers, dams, lakes, reservoirs, and other related water structures. However, as the global population increases, there is a corresponding increase in demand for water to fulfill various needs such as household, municipal, agricultural, and industrial. Undoubtedly, the assessment of water resources serves as an essential prerequisite for fostering sustainable development and effective management of water resources on a global scale (Kodoatie & Sjarief, 2010).

Hydrologic models have turned out to be crucial tools in assessing water resources. Understanding hydrological responses to Land Use and Land Cover (LULC) change becomes essential for the sustainable utilization of water resources and local ecological preservation of any catchment area. Hydrological modeling is carried out to understand this complex interaction and conceptualize and investigate the relationships among human activities, climate, and water resources. A river basin-scale model called the Soil and Water Assessment Tool (SWAT) that integrates GIS technology was established to measure the effects of land management techniques in substantial, intricate watersheds. Moreover, it improves the accuracy of generated results for water discharge from rainfall and basin physical characteristics. Input data like soil, land use, and slope of the study area were input into the model to simulate various physical processes in the basin. A graphical user interface is created via GIS and SWAT (Young et al., 1994). This study aims to develop a hydrological model using GIS and SWAT to assess the water yield of the Taguibo River Watershed.

METHODS

Study Area

The Taguibo River Watershed Forest Reserve (TRWFR) is located at Barangay Anticala, Butuan City (Figure 1). It encompasses approximately 4,367.44 hectares of public land in Butuan, RTR and Cabadbaran in the province of Agusan del Norte, with most of the land located in the city of Butuan (Moriarty et al., 2005). The watershed has a Type II climate, with rainfall spreading evenly throughout the year. This study was conducted within the TRWFR near the Taguibo Aquatic Solutions Corporation (TASC) reservoir as a sampling site for the study.
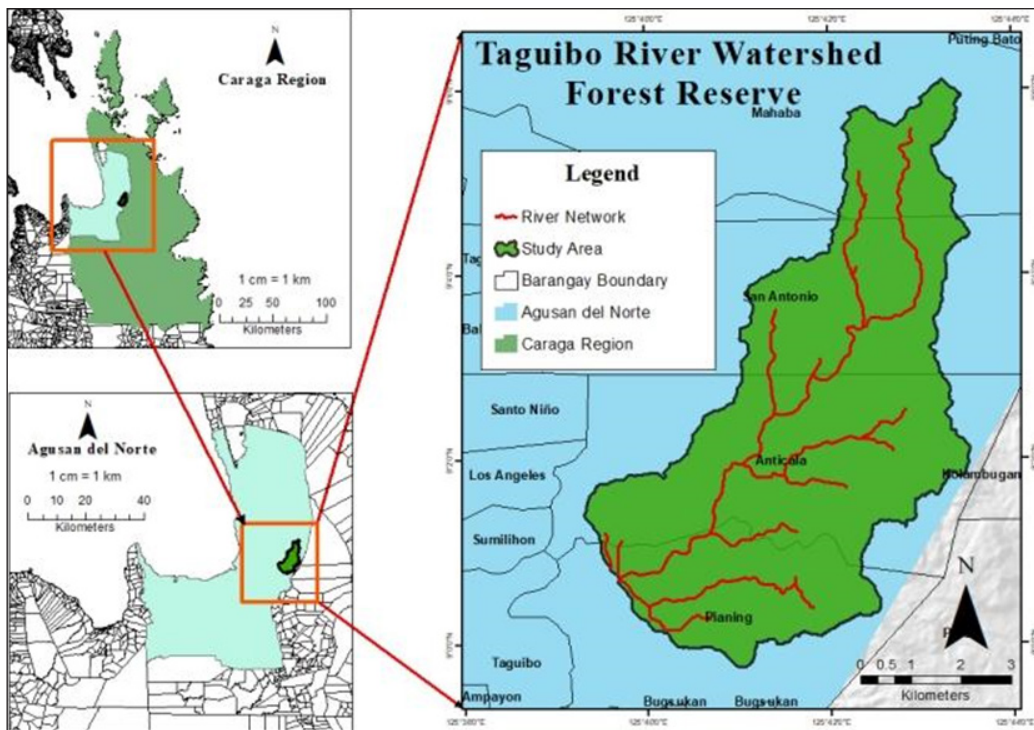
Figure 1. Map of the study area

Methodological Framework of the Study

Several methods were employed to set up the SWAT model, including data gathering, data processing, Hydrologic Response Unit (HRU) analysis, inputting the data into the SWAT model, running the model, and calibrating and validating the model. Figure 2 provides a visual representation of the methodology to simulate the hydrological processes of the Taguibo River Watershed Forest Reserve.

Data Collection

This study collected the following types of datasets, which were vital to processing and conducting the study's approaches. These were secondary data from different institutions. The datasets used for simulation in the SWAT model are presented in Table 1.

Digital Elevation Model

SWAT's automated watershed delineation feature produced the watershed's boundary. This feature employs the DEM data to recognize the flow direction and accumulation and establish a flow accumulation grid. After selecting an outlet point, the tool traces the upstream flow paths, creating the watershed boundary.

Aljon Ente Bocobo, Arnold Gemida Apdohan, Antonietto Ortega Cacayan Jr., Kenneth John Peña Lajera and Febe Hyacinth Andoy Simbolas
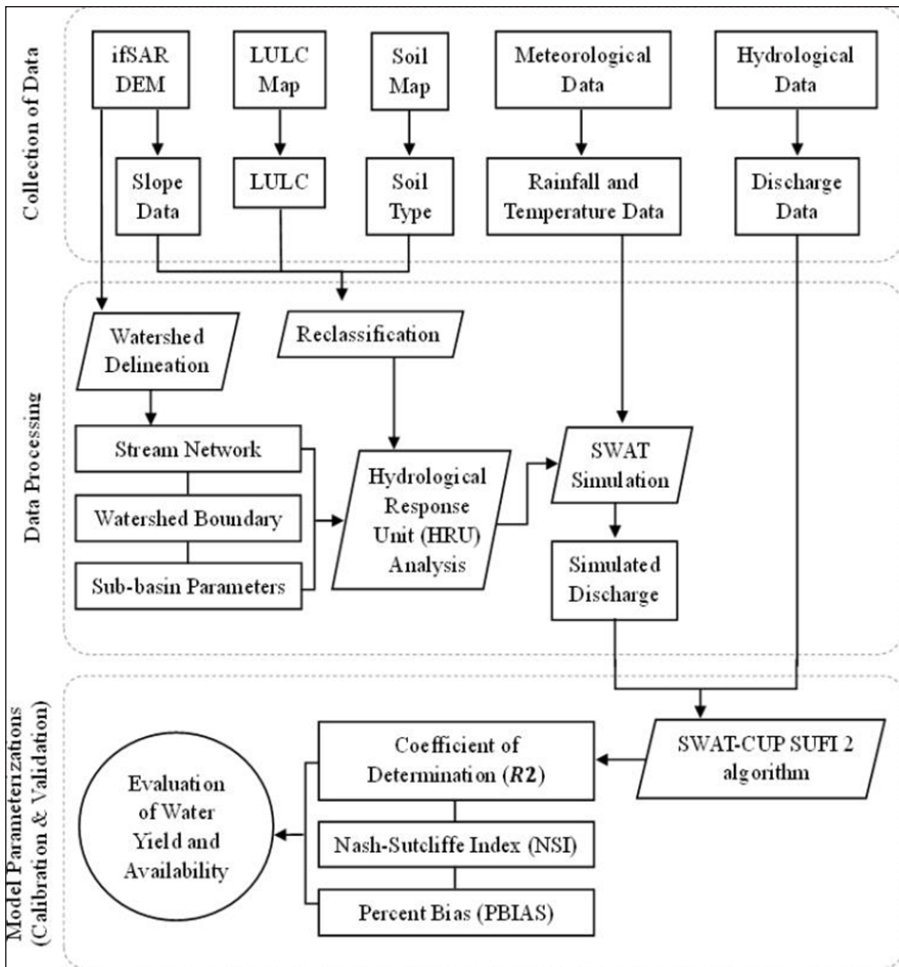
Figure 2. Flow diagram of the methodology

Table 1

Datasets used for simulation in the SWAT Model

DATASETS	SOURCE
Digital Elevation Model (DEM)	Mines and Geosciences Bureau
Land Use Land Cover (LULC) Map	CSU-CReATe (Center for Resource Assessment, Analytics and Emerging Technologies) generated using the Landsat OLI images
Soil Map	Bureau of Soil and Water Management (BSWM)
Weather Data (precipitation and minimum/maximum temperatures)	NASA Power	Data Access Viewer (power.larc.nasa.gov/data-access-viewer)
Discharge Data (Observed)	Butuan City Water District (BCWD) through CSU-CReATe (Center for Resource Assessment, Analytics and Emerging Technologies)

Slope Map

A slope map was derived from the DEM to define the Hydrological Response Unit, HRU. The slope map was generated by calculating the slope angle of the terrain using the DEM data.

Land Use Land Cover Map

The map was generated using Landsat 8 OLI images, which have a resolution of 30 meters and a supervised Support Vector Machine (SVM) classifier. The overall accuracy of the map was determined to be 96.6%. The map was used to identify and classify the different types of land cover in the study area. The land use land cover classification was based on the different spectral signatures obtained from the satellite images.

Soil Map

The soil map classified the soil into different types and contained information about the soil characteristics of the study area. This map was used as input while defining land use, soil, and slope for the HRU analysis in the SWAT modeling. This step was essential in identifying the different HRUs based on the soil type and slope of the land, which ultimately helped stimulate the study area's hydrological processes.

Meteorological Data

Weather Data

The historical daily weather data for the temperature and precipitation of the study area from 2012 to 2021 (a 10-year duration) were downloaded from NASA Power Data Access Viewer (power.larc.nasa.gov/data-access—viewer), as presented in Table 2. The data can also be acquired through government weather stations like the Philippine Atmospheric and Geophysical Service Administration (PAGASA).

SWAT needed daily climate and weather information gleaned from measurable data sets or produced by a weather generator model. The model needs precipitation, temperatures, relative humidity, wind speed, and solar radiation data.

Table 2
Monthly weather data for 2021

Months	WEATHER DATA		
	Minimum Temperature (°C)	Maximum Temperature (°C)	Precipitation (mm)
January	19.37	30.08	659.18
February	20.30	32.01	432.42
March	20.10	31.81	348.05

Table 2 (*continue*)

Months	WEATHER DATA		
	Minimum Temperature (°C)	Maximum Temperature (°C)	Precipitation (mm)
April	21.05	32.73	213.06
May	22.14	32.89	396.48
June	21.76	32.94	187.50
July	22.00	32.95	267.74
August	22.01	32.80	212.17
September	21.79	33.76	282.91
October	21.14	32.94	435.15
November	21.68	31.66	567.30
December	21.12	30.37	664.57

Hydrological Data (Observed Discharged Data)

The observed discharge data was collected from a stream located at 8.9786° N, 125.6287° E, situated 150 meters upstream of the TASC Hydro Dam outlet. It is positioned before the dam's outlet along the water flow path. This location is commonly used to measure discharge (water flow rate) and monitor the inflow into the dam. The observed discharge data for the years 2010, 2011, 2012, and 2013 were acquired from Butuan City Water District (BCWD) through CSU-CReATe. These data were used to calibrate and validate the model using the SWAT-CUP - SUFI-2 optimization algorithm.

Data Processing

The first step was to process the DEM using ArcMap 10.3 software. The study area's watershed boundary was extracted by clipping the DEM data using the clip command tool within the ArcMap interface, which had the same coordinate system. The slope map was then generated by using the slope command tool in the ArcMap 10.3 interface. The land use map, soil map, weather data (precipitation and minimum/maximum temperatures), and discharge data (observed) were used as inputs to generate the model, and different maps were created that were essential for the study. The data processing was necessary to convert raw data into usable input formats for the model.

Hydrological Response Unit Analysis

HRU analysis combined three categorical variables- soil type, slope, and land- to create HRUs. The slope spatial analysis tool in Arc Map 10.3 software was used to determine the slope of a watershed from a DEM. The tool converts the elevation into a slope projection using the percent slope using the DEM file as the input raster. The subsurface lateral water movement, flow buildup and routing, as well as the sediment yield for each sub-basin,

were filled in by this parameter for SWAT (Arnold et al., 1998). The unique combinations of land use, soil type, and slope were used to develop the HRUs.

SWAT Input

A scale model of a river basin or watershed is called SWAT, or Soil and Water Assessment Tool. Dr. Jeff Arnold created it for the USDA Agricultural Research Service (ARS). It was created to predict how land management methods in sizable, complicated watersheds with a range of soil types would affect water, sediment, and agricultural chemical outputs. A watershed is divided into multiplex sub-watersheds in SWAT, and these are then further divided into hydrologic response units, HRUs, which are made up of homogeneous topographical, soil, and management characteristics. Water balance is said to be the driving force behind all SWAT activities because it influences plant growth and the flow of sediments, nutrients, pesticides, and pathogens (Arnold et al., 2012). This model can mimic several important hydrologic processes, such as evapotranspiration, surface runoff, infiltration, percolation, shallow and deep aquifer flow, and channel path (Arnold et al., 1998). SWAT can simulate various hydrologic processes, including canopy storage, surface runoff, infiltration, evapotranspiration, lateral flow, tile drainage, and water redistribution within the soil profile (Abbaspour et al., 2015). The hydrologic cycle in the SWAT model is simulated by utilizing the water balance as expressed in Equation 1.

$$SW_t = SW_o + \sum_{i=1}^{n} \left(R_{day} - Q_{surf} - ET - W_{seep} - Q_{gw} \right) \qquad [1]$$

where SW_t is the final soil water content (mm), SW_o is the initial soil water content on day i (mm), t is the time (days), R_{day} is the amount of precipitation on day i (mm), Q_{surf} is the amount of surface runoff on day i (mm), E_a is the amount of evapotranspiration on day i (mm), W_{seep} is the amount of water entering the vadose zone from the soil profile on day i (mm). Q_{gw} is the amount of return flow on the day i (mm).

Watershed Delineation

In constructing the model, the generated DEM was first used to delineate the watershed by generating sub-watersheds using the ArcSWAT automatic watershed delineator toolkit. The output includes calculating the stream network, determining the watershed boundary, and calculating the sub-basin parameters.

SWAT Simulation

Given that the raw input data are complete, the setup and running of the model simulation were completed. SWAT may then instantly check for any issues after that. Using SWAT Output Viewer or ArcMap 10.3, the output data from the SWAT project was viewed and

displayed on time series graphs or themed maps. One may view daily, monthly, and yearly output parameters broken down by watershed, HRU, sub-basin, and reservoir.

Water Yield

In the output of the SWAT model, the total water yield can be viewed and presented in daily, monthly, yearly, or average values for each sub-basin or the whole watershed. Equation 2 is used to represent water yield in the SWAT model:

$$WYLD = SURQ + LATQ + GWQ - TLOSS - pond\ abstractions \quad [2]$$

where WYLD is the water yield in millimeters; SURQ is the contribution of surface runoff to streamflow in millimeters; LATQ is the contribution of lateral flow to streamflow in the watershed on a given day, month, or year in millimeters; GWQ is the contribution of groundwater to stream in the watershed on a given day, month, or year in millimeter; and TLOSS is the transmission loss, or the amount of water lost from tributary channels in the HRU. The entire HRU Land Use Soils Report drainage area was multiplied by the Water Yield to calculate the volume. Given that the Butuan City Water District taps and distributes surface water from this area of the watershed, the water yield was computed for this study (Ayivi & Jha, 2018).

Calibration and Validation of the Model

Calibration is estimating model parameters that cannot be measured directly. It can be an automated process, a manual procedure, or a combination of these. The goal of calibration is to determine the model's performance potential. Refsgaard and Storm (1996) provided a methodical approach for model calibration and validation. The method for calibrating the SWAT was outlined from 2003 to 2013 (11 years); however, in this study, calibration was done from 2003 to 2008. The same validation procedures were used for the watershed from 2009 to 2013. Three performance indicators were employed in this study: percent bias (PBIAS), Nash-Sutcliffe Index (NSI), and coefficient of determination (R^2).

SWAT -CUP SUFI 2 Algorithm

The streamflow, used as a reference to calculate other water flows indirectly, was the primary measurable metric of water flow in the watersheds (Farzana et al., 2019). Streamflow is one of the measurements used for calibration and validation in hydrology modeling (Saleh et al., 2000). Other factors like evapotranspiration, groundwater recharge, and surface runoff, among others, are challenging to assess and have data only available at specific periods in time and space (Bracmort et al., 2006).

The algorithm for Sequential Uncertainty Fitting (SUFI-2) is an approach that uses the chosen parameter ranges during an iteration process consisting of 300–1000 simulations to attempt to capture most of the measured data within the model's 95% prediction uncertainty (95PPU) (Abbaspour et al., 2015). Through trial runs, automatic calibration procedures were carried out using a prior parameter analysis (10–100 simulations). The sensitivity analysis of stream flow-related variables throughout this trial helped to identify the final values chosen for calibration and validation. For both processes, homogeneous flow time series durations were selected to offer consistent statistical samples and to evaluate the more recently available data. Nevertheless, due to cumulative model input uncertainties, a good correlation during validation may provide an inconsistent output (Bracmort et al., 2006).

Coefficient of Determination (R^2)

The coefficient of determination (R^2) indicates the percentage of variance in derived data that the model experiences. R^2, as expressed in Equation 3, is the most used criterion for evaluating a model's performance.

$$R^2 = \left(\frac{\sum_{i=1}^{n}(O_i - \bar{O})(P_i - P)}{\sqrt{\sum_{i=1}^{n}(O_i - \bar{O})^2}\sqrt{\sum_{i=1}^{n}(P_i - P)^2}} \right) \quad [3]$$

where O_i is the observed flow discharge at the time I, $\bar{O}$ is the average observed flow discharge, P_i is simulated flow discharge at time I, P ˙, P is the average simulated flow discharge, and n is the number of registered flow discharge data. Table 3 lists the general performance rating criteria for the calibration and validation of this model (Farzana et al., 2019).

Table 3
Performance rating for R^2

Performance Rating	R^2
Very Good	$R^2 > 0.70$
Good	$0.60 < R^2 \leq 0.70$
Satisfactory	$0.50 < R^2 \leq 0.60$
Unsatisfactory	$R^2 > 0.50$

Nash-Sutcliffe Index

The Nash-Sutcliffe Index, NSI, value represents how well the 1:1 line fits the observed versus simulated data. Equation 4 calculates NSI.

$$NSI = 1 - \frac{\sum_{i=1}^{n}(O_i - P_i)^2}{\sum_{i=1}^{n}(O_i - \bar{O})^2} \qquad [4]$$

Where the notations indicate the same meaning as described before, Table 4 provides the performance ratings for this model's NSI, which are classified at various levels (Bracmort et al., 2006; Saleh et al., 2000).

Table 4
Performance rating for NSI

Performance Rating	NSI
Very Well	$NSI > 0.65$
Adequate	$0.54 < NSI < 0.65$
Satisfactory	$NSI > 0.50$

Percent Bias

The percent bias, PBIAS, measures whether the simulated data is greater or smaller than the observed data (Gupta et al., 1999). A PBIAS score of 0 implies accurate model simulation. Positive values suggest that the model was underestimated, whilst negative values indicate that the model was overestimated (Gupta et al., 1999). Equation 5 is used to determine PBIAS:

$$PBIAS = \frac{\sum_{i=1}^{n}(O_i - P_i)}{\sum_{i=1}^{n} O_i} \times 100 \qquad [5]$$

where the notations indicate the same meaning as described before.

RESULTS AND DISCUSSION

Watershed Delineation

Watershed delineation divided the project area into 26 sub-basins, each with a topographic report containing information such as the maximum, minimum, mean, and standard deviation of elevation. The total project area has a maximum elevation of 1883.98 m and a minimum of 93.0351 m above mean sea level. The mean elevation for the area is 890.33 m, and the standard deviation is 395.865 m. The output from the watershed delineation process also included the reach, sub-watershed, and sub-basin boundaries. The map in Figure 3 shows the delineated upstream watershed, including the watershed boundary, basins, longest path, and its reach. The generated sub-basin boundaries provided an understanding of the hydrological system of the study area, which is critical in the simulation of water resources in the SWAT model. Overall, the delineation of the watershed and sub-basins provides

essential information for water resource management and conservation in the study area (Li et al., 2021; Shivhare et al., 2018).
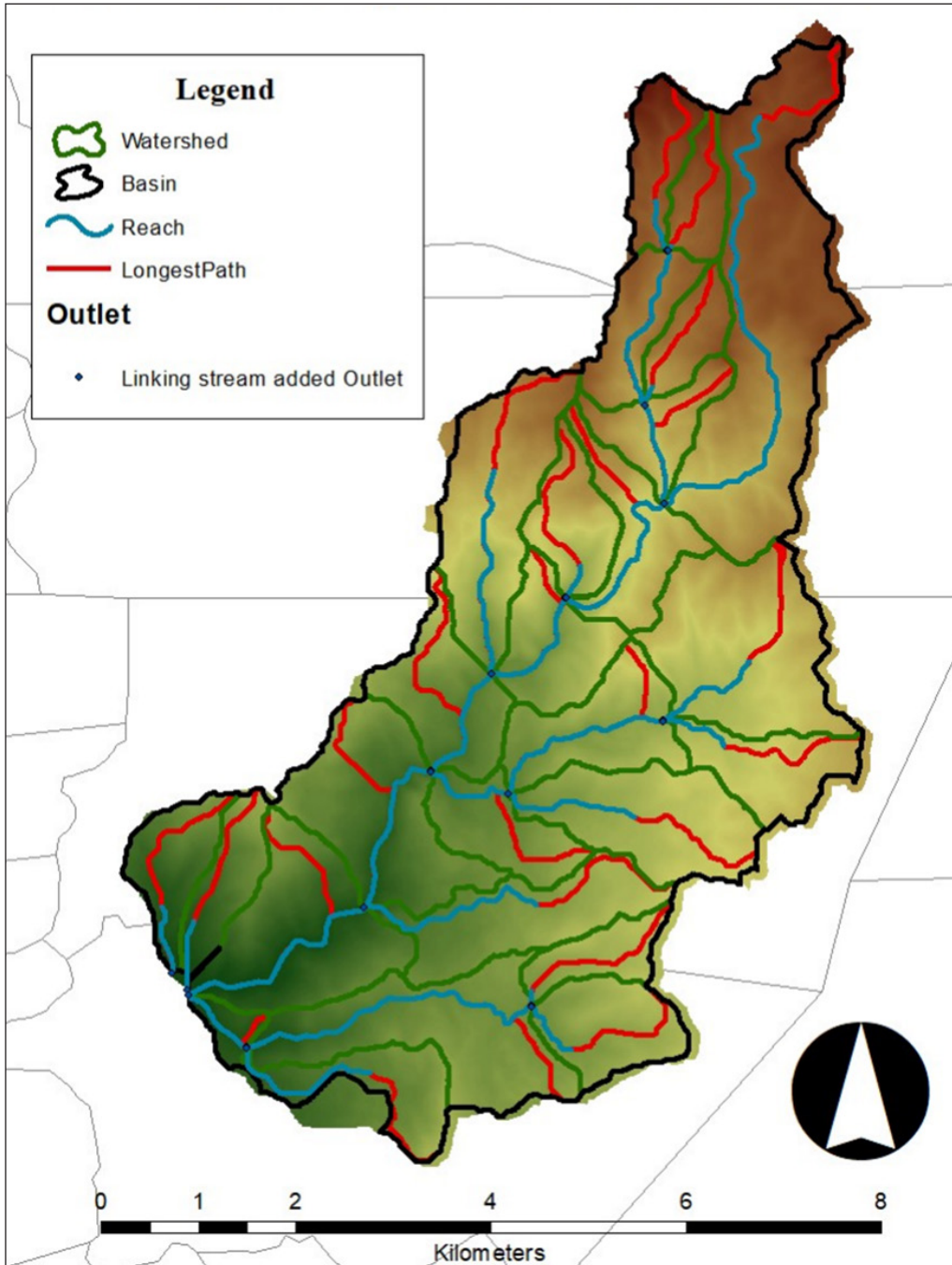
Figure 3. Delineated upstream watershed

Hydrological Response Unit Results

The hydrological response unit, HRU, included the region for the study area's upstream watershed, 4105.43 hectares (10144.7303 acres). Table 5 contains the reclassified land use, soils, and slope statistics during the HRU process.

Table 5
Hydrological response unit (HRU) results

	Land Cover Classes	SWAT Classes	Area (ha)	Watershed Area (%)
Land Use	Agricultural Area	AGRL	65.17	1.59
	Palm	OILP	333.25	8.12
	Grassland	FRSE	247.98	6.04
	Mixed Vegetations	PAST	30.71	0.75
	Forest	FRST	3398.61	82.78
	Urban	URBN	25.05	0.61
	Barren	BARR	0.51	0.01
	Water	WATR	4.15	0.10
Soil	Mountain Soil (undifferentiated)	MTSOILUND	2065.33	50.31
	Malalag Silt Loam	MALALAGSL	2025.38	49.33
	Camansa Clay	CAMANSAC	14.72	0.36
Slope (%)	50–9999		1670.79	40.70
	30–50		1396.72	34.02
	20–30		610.33	14.87
	10–20		368.67	8.98
	0–10		58.93	1.44

Figure 4 visually represents various land use classes in the watershed. The study utilized a land LULC map to identify and classify different land cover types in the watershed area. The LULC map was generated using satellite images and a supervised SVM classifier. Eight land use classes were identified and mapped out in this area. The percentage of the total area covered by each land use class is also in the figure. Agricultural land covers 1.59% of the entire watershed area, palm covers 8.12%, and grassland covers 6.04%. Pasture, on the other hand, covers only 0.75% of the site. The residential land use class covers only 0.61% of the watershed area, while barren land covers only 0.01%. Water covers 0.10% of the total area. Notably, the forest land use class dominates the entire area of the watershed, covering 82.78%. It implies that a mix of different forest types covers most of the land in the watershed; this can have important implications for the local ecosystem, such as providing habitat for wildlife, contributing to local climate regulation, and protecting soil from erosion.
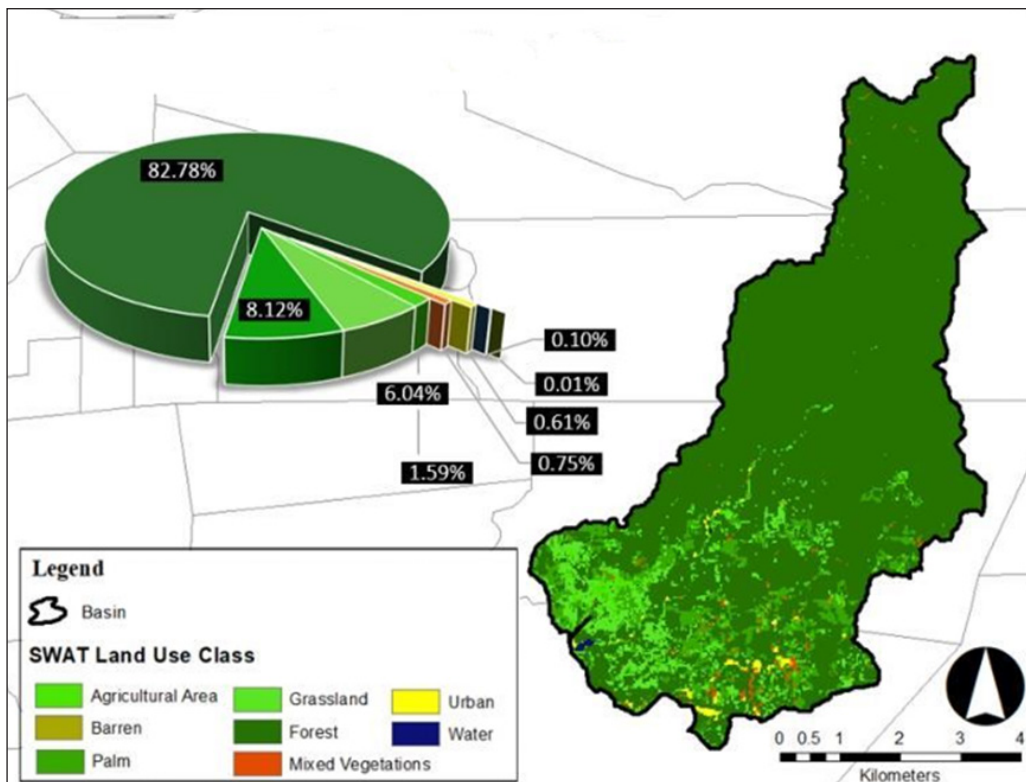
Figure 4. Reclassified land use map

Figure 5 depicts the characteristics of different types of soils found in a mountainous region, along with the corresponding watershed area. The three soil types mentioned in this figure are Mountain Soil (undifferentiated), Malalag Silt Loam, and Camansa Clay. The Mountain soil covers 50.31% of the watershed, while Malalag silt loam covers 49.33% of it. The remaining 0.36% of the watershed comprises Camansa clay.

Figure 5 also suggests that most of the soil in the watershed belongs to hydrologic soil group B, characterized by loamy and silty loamy soils (Galintao & Santillan, 2020). This soil group has moderate infiltration rates, water storage capacity, and runoff potential. These characteristics can influence how water moves through the soil, affecting factors such as erosion, groundwater recharge, and water availability for plants and animals. This information can help understand the region's hydrology and ecology and make wise land use decisions.

Figure 6 displays the essential information about the classes of the slope and their respective watershed area. The data are presented into five distinct categories. The first category, which covers the range of slopes between 50 and 9999, has the highest percentage, 40.70%; this suggests that a significant portion of the watershed area has a steep slope, which could impact water flow and lead to erosion. The second category, which covers the
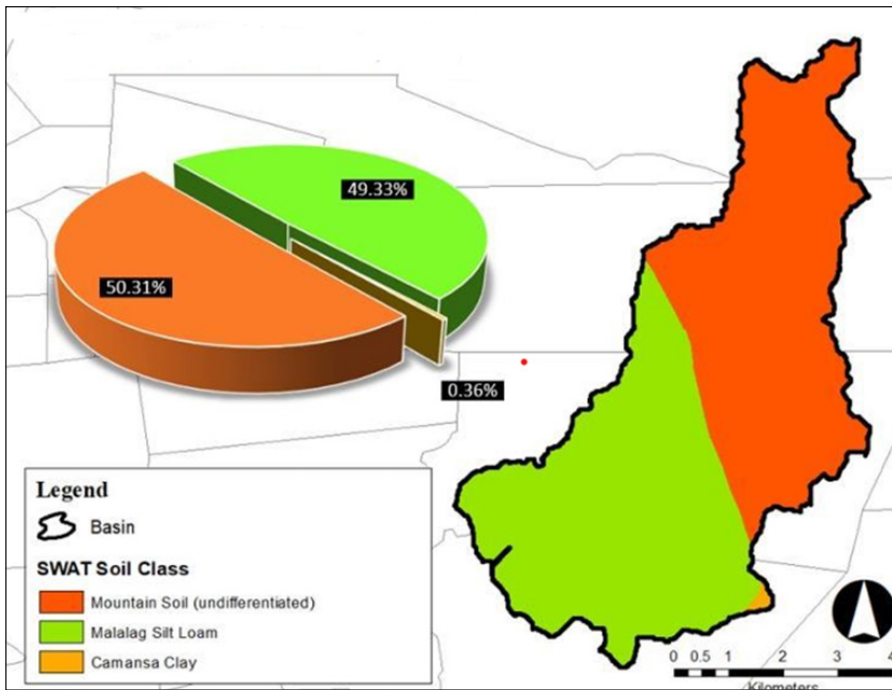
Figure 5. Reclassified soil map
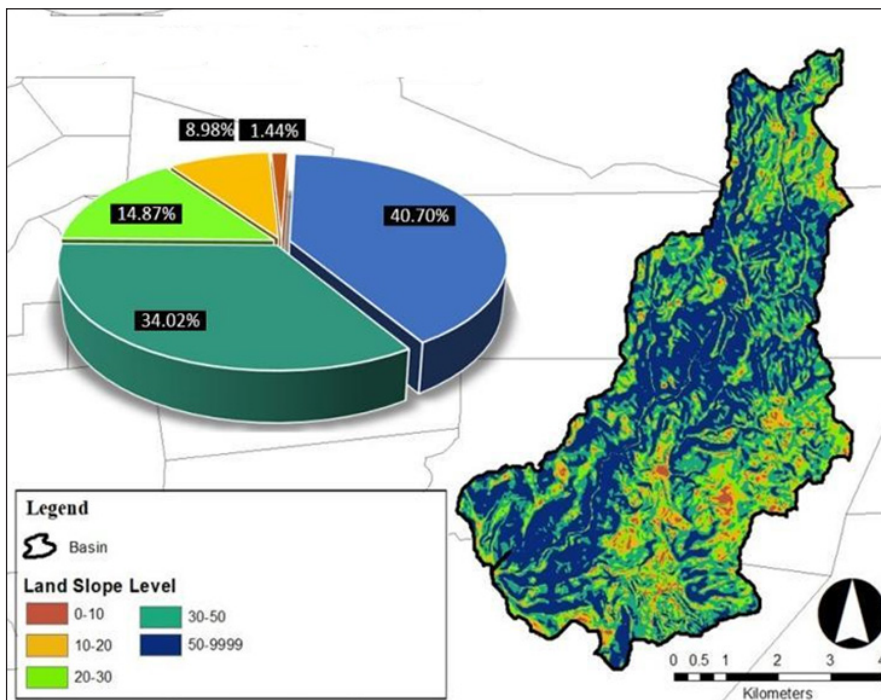
Figure 6. Reclassified land slope map

range of slopes between 30 and 50, has a percentage of 34.02%; this is also a significant percentage and indicates that a large portion of the watershed area has a moderate slope. The third category, which covers the range of slopes between 20 and 30, has a percentage of 14.87%; this indicates that a smaller portion of the watershed area has a moderately low slope. The fourth category, which covers the range of slopes between 10 and 20, has a percentage of 8.98%; this is a relatively small percentage and suggests that a small portion of the watershed area has a low slope. Finally, the fifth category, which covers the range of slopes between 0 and 10, has the smallest percentage of 1.44%; this suggests that only a tiny portion of the watershed area has a nearly flat slope. The information on the distribution of slopes (Figure 6) can be used to understand the potential impact of water flow and erosion on the landscape. It can help inform decisions about land use and conservation efforts.

The map shown in Figure 7 shows the full HRU result, basin, and its reach. The HRU is a combination of the soil data, land use land cover data, and slope data that was derived from the DEM of the study area. The forest dominated the entire watershed with about 82.78%. Moreover, it has loamy and silty loamy soils that have moderate infiltration rate, water storage capacity, and runoff potential. Also, with 40.70%, a significant portion of the watershed area has a steep slope that can affect water flow and lead to erosion.

SWAT Output Data

The SWAT simulation generates various output files, including reach, sub-basin, and HRU outputs, which could be displayed as daily, monthly, annual, or average yearly values. For each area of the watershed that it is assigned to, each output file comprises a summary of the data. The output is important for this study because it provides an overview of the water resources of the watershed and includes simulations of water yield, evapotranspiration (ET), surface runoff, percolation, lateral flow, groundwater flow (return flow), transmission losses, ponds, and other hydrological components Khoury et al. (2023). Additionally, only the water yield from sub-basins 1 through 26, encompassing the Taguibo River Watershed, was used in this analysis from 2010 to 2021 because the watershed was separated into sub-basins.
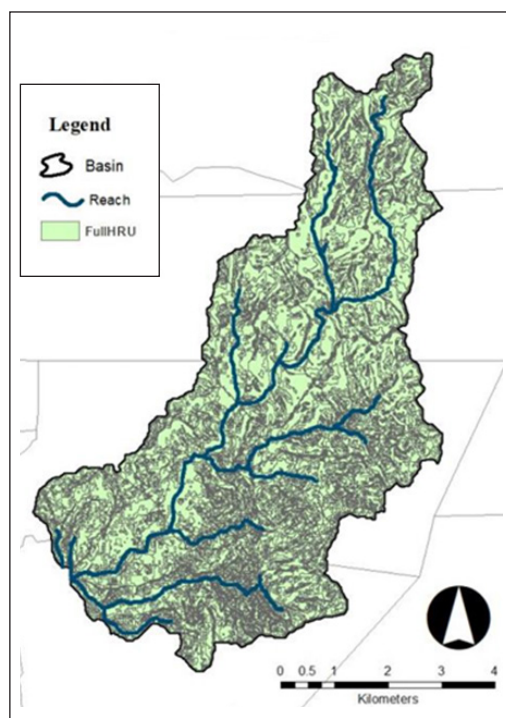
Figure 7. Hydrological response unit result
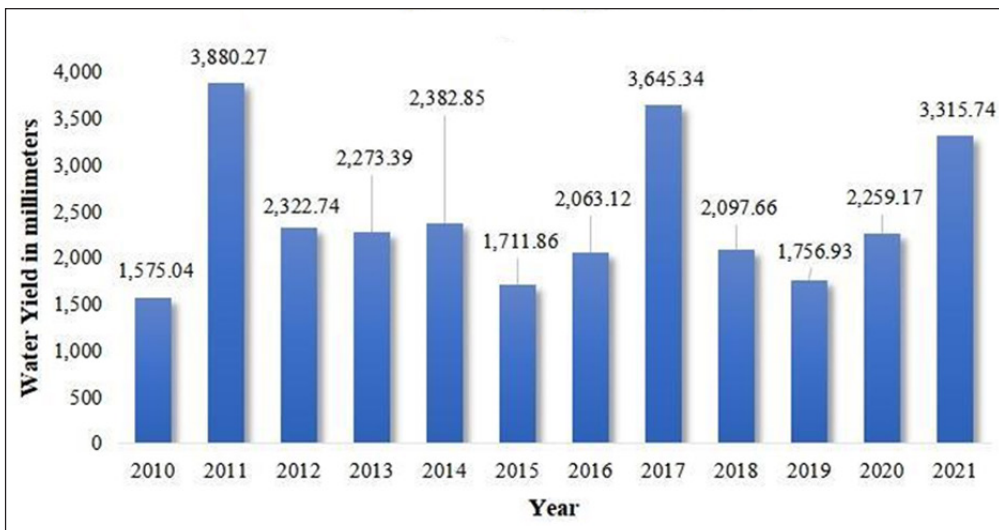
Figure 8. Water yield of the TRWFR at different years

Figure 8 displays the water yield graph for the upstream watershed from 2010 to 2021; this graph provides an important visual representation of the trend of water yield values over time to understand the changes in the watershed. Upon close examination, it becomes clear that the trend of the water yield values has changed significantly annually, meaning that the water produced yearly by the watershed was inconsistent. One factor that contributed to these alterations was precipitation. Changes in precipitation patterns can significantly impact the amount of water produced by the watershed Guo et al. (2023). For example, if there is a drought, the amount of water produced will likely be lower than if there is a period of heavy rain. Other factors such as changes in land use, temperature fluctuations, and natural events like wildfires may also play roles in these alterations. It is crucial to study these factors to understand the watershed's dynamics better and to develop effective strategies for managing its resources.

Figure 9 presents the spatial distribution of water yield levels in an upstream watershed for the years 2010, 2013, 2015, and 2018, illustrating the variability in water availability over time. Between 2010 and 2013, the watershed experienced an overall increase in water yield, indicating higher precipitation or changes in watershed conditions that enhanced water retention. However, a notable decrease in water yield occurred in 2015, likely due to a slight reduction in precipitation across the watershed area. By 2018, water yield levels had increased again, indicating a recovery that may be linked to improved precipitation rates or other hydrological factors. In contrast, Figure 10 highlights a significant rise in water yield in 2021, which can be attributed to a marked increase in precipitation patterns within the watershed, as shown in Figure 11.
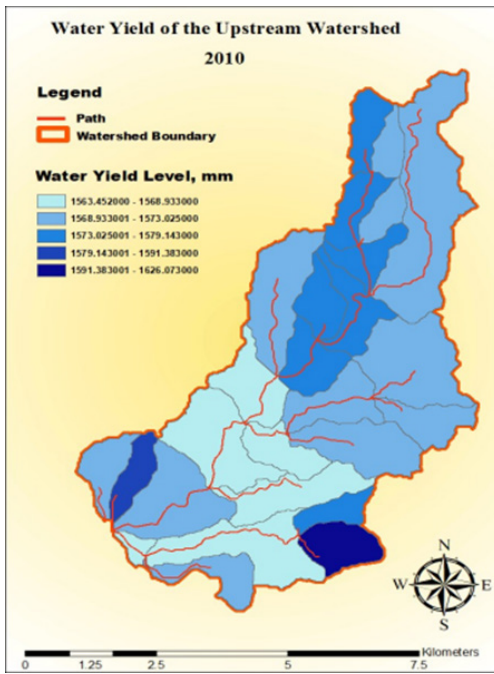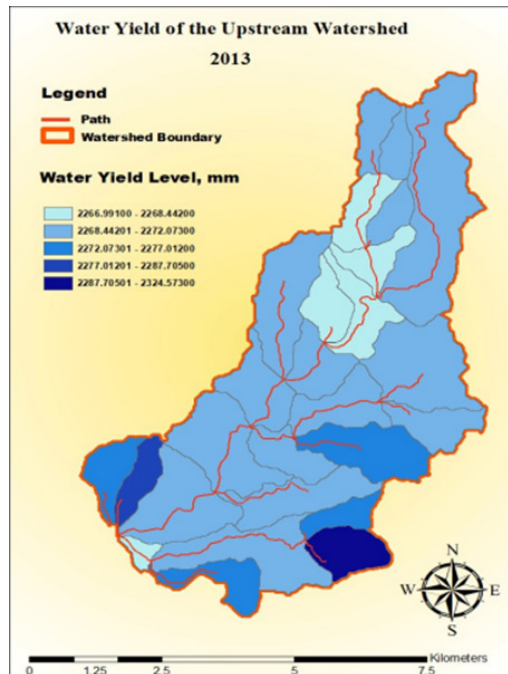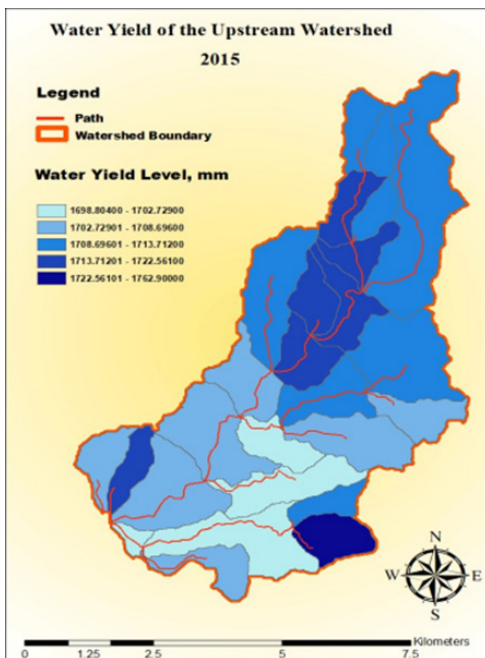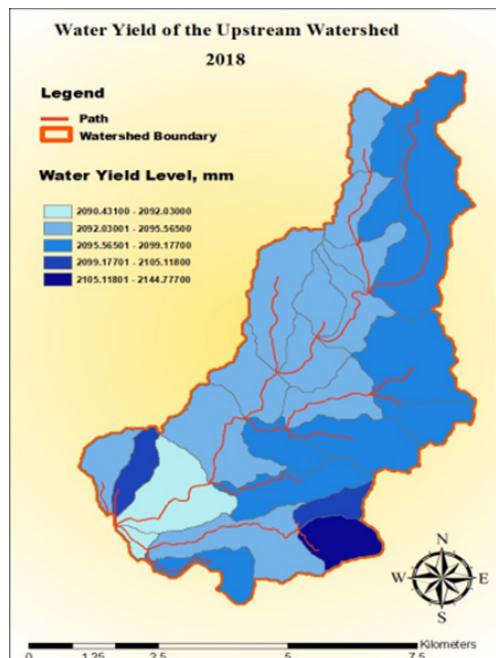
Figure 9. Upstream water yield: (a) 2010; (b) 2013; (c) 2015; (d) 2018
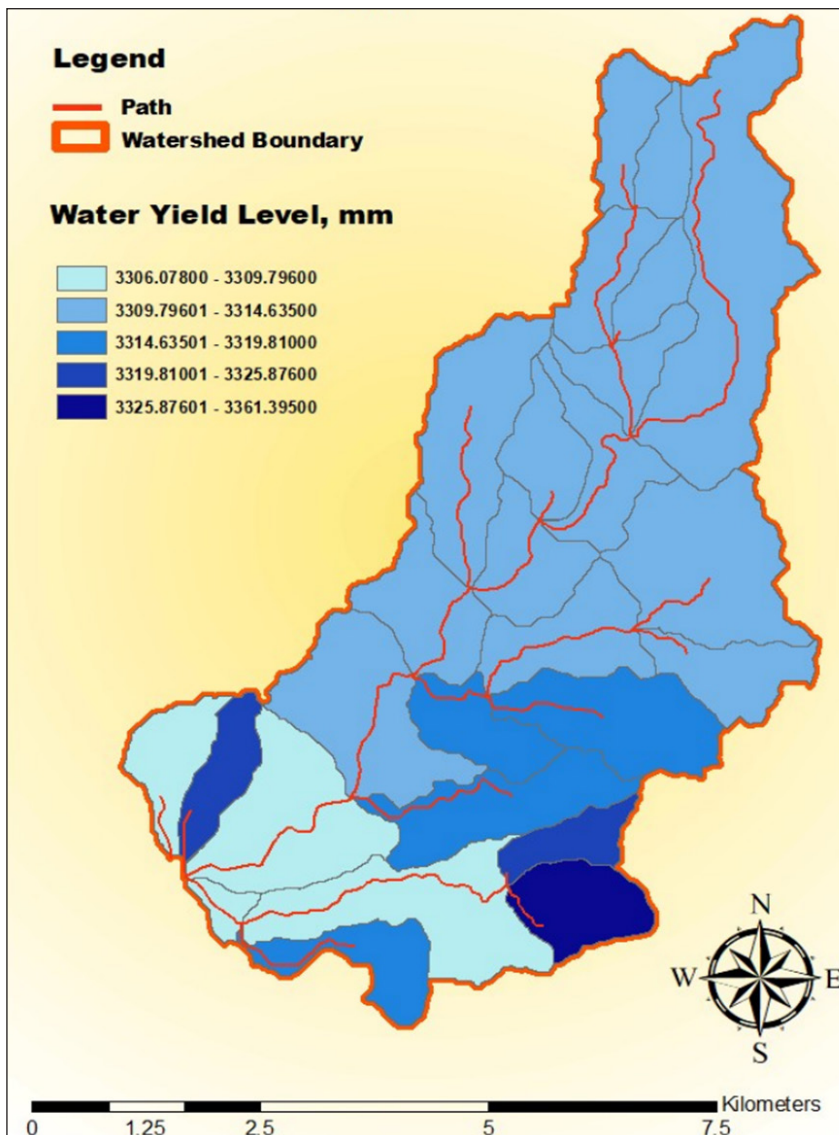
Figure 10. Upstream water yield 2021

Relationship Between Water Yield and Precipitation

Figure 11 illustrates the total annual water yield and precipitation from the year 2010 to 2021. The changes in flow in the catchment area rely on the variations of the precipitation Oda et al. (2024). The first year shows decreased water yield and precipitation, with almost 2000 mm of average water yield and annual precipitation between 2,000 mm and 4,000 mm. The following year, 2011, shows that the average water yield almost reached 4,000 mm, and its annual precipitation reached between 4,000 mm and 6,000 mm, the highest

reach in the past years. The years 2012–2016 have the least significant changes based on their average water yield and precipitation. There is a significant difference between 2016 and 2021.
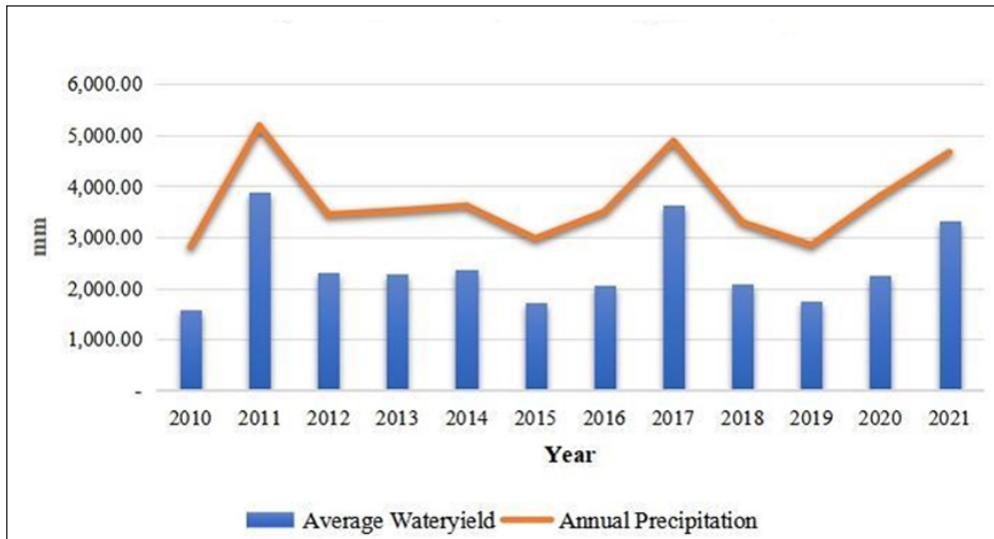
Figure 11. Relationship of water yield and precipitation

Comparison between Runoff Volume and Land Use Land Covers

Figure 12 illustrates the average monthly streamflow data for the years 2013, 2015, 2018, and 2021 based on simulations from the SWAT model. The study area experiences a tropical Type II climate, as classified by the Philippine Atmospheric, Geophysical and Astronomical Services Administration (PAGASA), characterized by a generally even distribution of rainfall throughout the year, with no distinct dry season. This climate features wet and very wet periods rather than clear wet-dry seasonal divisions. However, the region does undergo a phase of high precipitation from November to February, often accompanied by heavy rain showers. From March to October, the remaining months receive relatively lower precipitation levels. When comparing across years, there are notable differences. In 2013, streamflow starts high but sharply drops from March to May, with a moderate peak in November; however, its peak values are lower compared to other years. The year 2015 has the lowest overall streamflow, especially from May through August, reflecting possibly drier conditions. The year 2018 follows a similar trend to 2013 but maintains relatively higher values from March to June without any extreme peaks. Meanwhile, 2021 stands out with significantly higher streamflow throughout the year. It suggests an unusually high influx of water in late 2021, possibly due to heavy rainfall or other hydrological factors.

Aljon Ente Bocobo, Arnold Gemida Apdohan, Antonietto Ortega Cacayan Jr., Kenneth John Peña Lajera and
Febe Hyacinth Andoy Simbolas
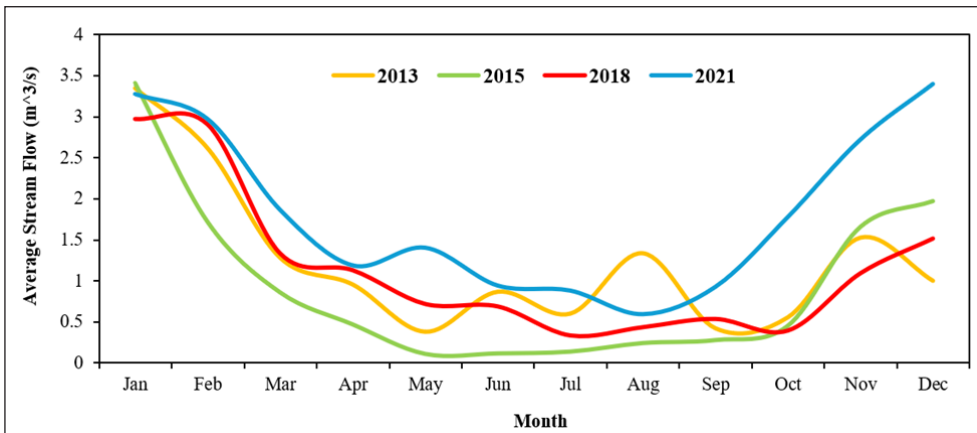
Figure 12. Simulated streamflow of the model for the years 2013, 2015, 2018 and 2021

Figure 13 illustrates the relationship between forest area and streamflow in 2013, 2015, 2018, and 2021. In 2013, the forest area was 2,483 ha, with a 1.24 m3/s streamflow representing the lowest forest area and a relatively high streamflow in the observed period. By 2015, the forest area had expanded to 3,039 ha, while streamflow decreased to 0.95 m^3/s, possibly due to increased water retention as forest cover grew and lower precipitation received that year (Figure 11). In 2018, forest area continued to increase, reaching 3,143 ha, with a slight rise in streamflow to 1.17 m^3/s. By 2021, the forest area reached 3,658 ha, and streamflow showed a substantial increase to 1,83 m^3/s. Despite the large forest area, this notable increase in streamflow suggests that other factors, such as higher precipitation or changes in hydrological conditions, may have contributed to the fluctuations in streamflow, particularly the significant increase observed in 2021.
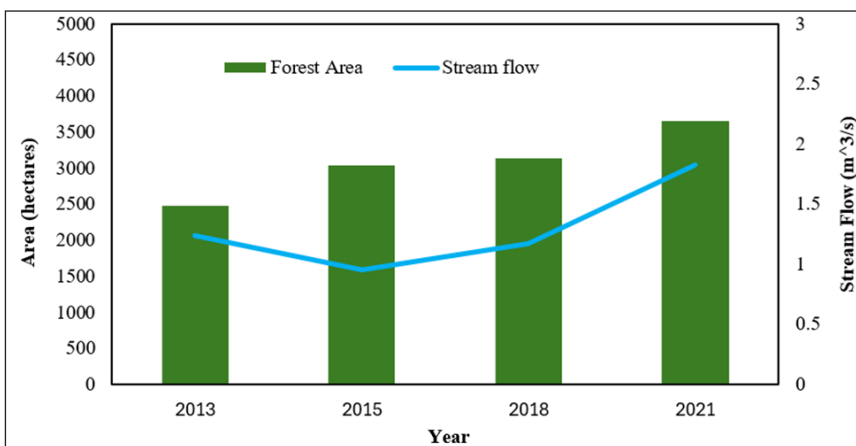
Figure 13. Forest area and its estimated streamflow Estimated streamflow in the watershed for the years 2013, 2015, 2018, and 2021

Model Calibration of LULC Year 2021

The result in Figure 14 compares the discharge of observed and predicted flows throughout the calibration period for two years (2010–2011). This study only used 2010 and 2011 as input years during calibration due to the insufficiency of the data acquired. These data served as the basis for the succeeding years that should be included in the calibration process. Figure 14 indicates the actual and simulated flow, denoted by blue and orange colors. The actual flow coincides with the simulated values. Moreover, the observed and simulated points intersect in April of 2010, July of 2010, December of 2010, March of 2011, and December of 2011.
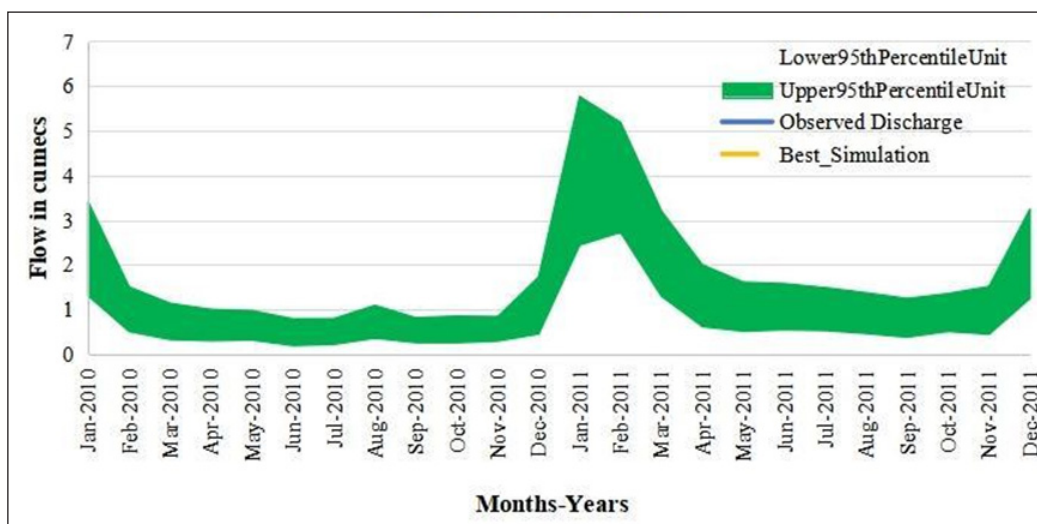
Figure 14. Comparison of the observed and simulated discharges during model calibration for two years (2010–2011)

Figure 15 illustrates the link between the observed and simulated discharges with R^2= 0.63, NSI = 0.33, and PBIAS = –29.9%. The observed and simulated flows have a good linear relationship. According to the NSI value of 0.33, the simulation results were adequate. A negative PBIAS value of -29.9% indicates a correct model simulation. The difference between the simulated and observed discharge data should be evaluated to see if the model is effective and how well it forecasts the actual water flows in a river or stream. The model's capacity to simulate water flows under various conditions can be trusted if the simulated discharge data agrees with the observed data.

Figure 16 compares observed and simulated discharges throughout the validation period from 2012 to 2013, represented by blue and orange lines. Due to the inadequacy of the collected data, the model was validated using only the input years of 2012 and 2013. The following years were expected to be incorporated into the validation procedure based on

these data. The observed and simulated values of the model during validation meet in most of the months throughout the years 2012 and 2013. It started to link together in January 2012 and started to disconnect in February 2012, and continues to correlate in April 2012, August to October 2012, early December 2012, late December 2012 to February 2013, July to August 2013, and late October 2013 to December 2013.
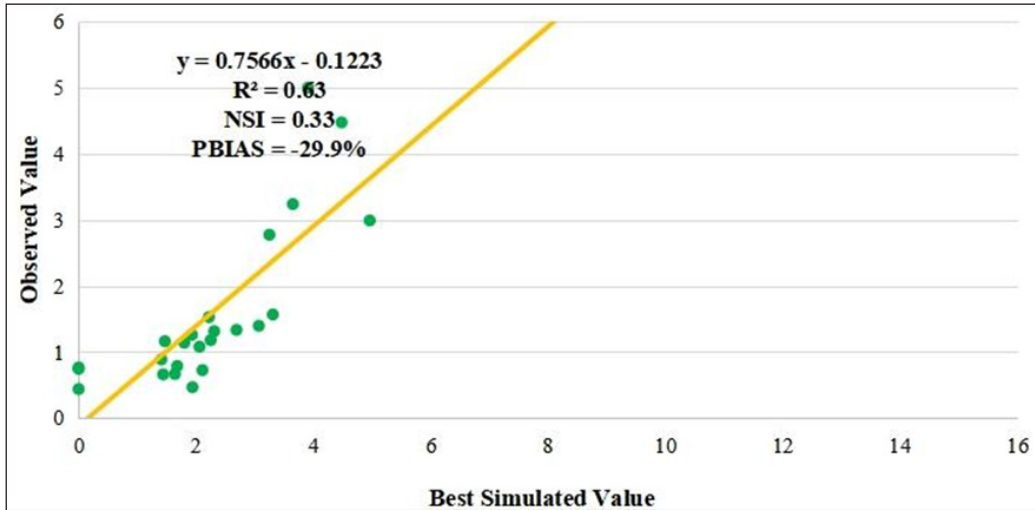
Figure 15. Relationship between the simulated and observed discharges during the calibration period
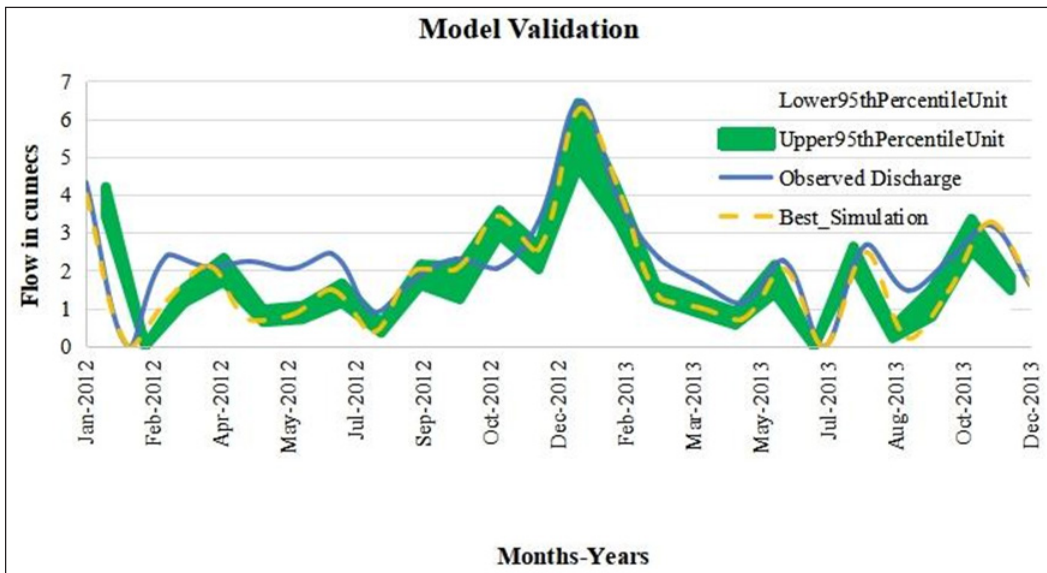
Figure 16. Comparison of the observed and simulated discharges during model validation for two years (2012–2013)

Model Validation of LULC Year 2021

In general, validation is a crucial stage in the creation of hydrological models in ArcSWAT. It improves water management decision-making, identifies model constraints, and increases the model's credibility by establishing trust in its capability to simulate water flows under various conditions (Koltsida et al., 2023).

The scatter graph in Figure 17 demonstrates the relationship between the simulated and observed discharges of the model during the validation period. Compared to the calibration period, validation acquired better results. In addition, it indicates that the observed and simulated flows have a good linear relationship with R^2 of 0.87 and NSI of 0.73, which means that the findings were satisfactory. A negative PBIAS value of –19% indicated a correct model simulation. It is essential to validate the relationship between the observed and simulated discharge data to guarantee that the hydrological model correctly predicts water flows in a river or stream. In addition to that, it also aids in evaluating model correctness, refines the model, gives decision-makers better data for managing water resources, and boosts trust in the model's dependability.
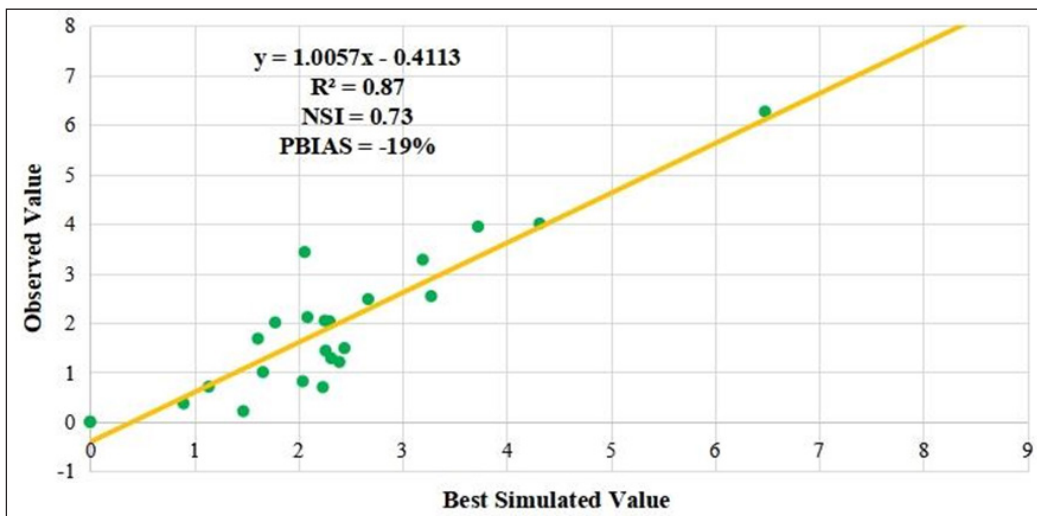
Figure 17. Relationship between simulated and observed discharges during the validation period

Comparison of calibrated and validated stream flows using different land covers for the years 2013, 2015 and 2018.

Figure 18 presents the calibration and validation results for streamflow simulations across three land use and land cover (LULC) years: 2013, 2015, and 2018. Each sub-figure represents stream flow simulation results for a specific LULC year, with the green shaded area showing the 95% uncertainty range, bounded by lower and upper confidence limits. The blue line indicates the observed discharge, representing actual recorded stream flow
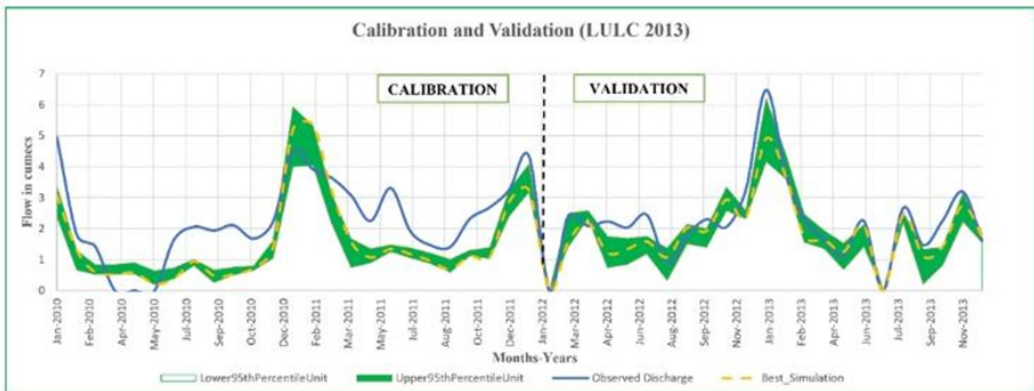
(a)
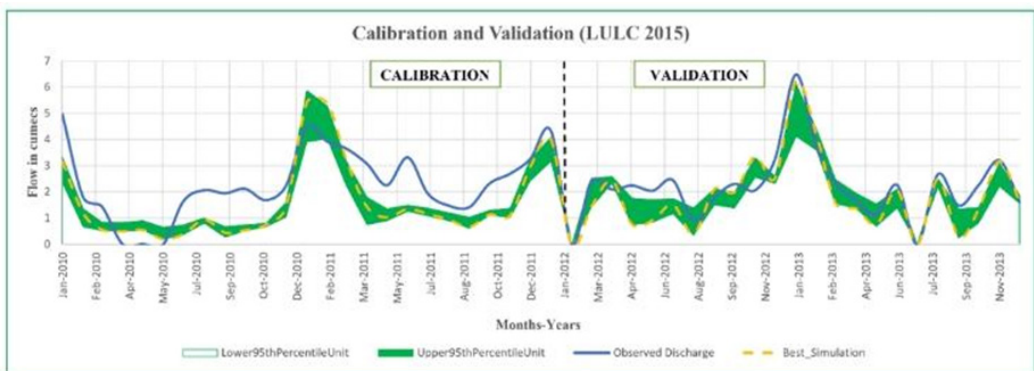
(b)
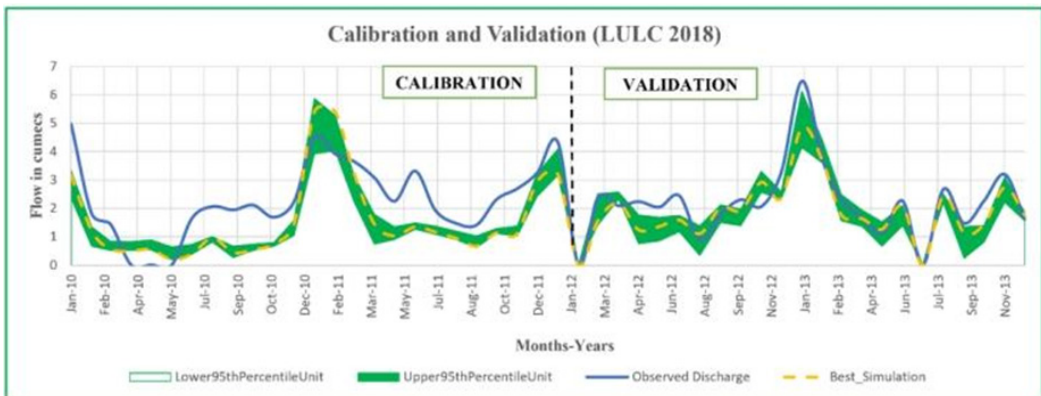
(c)

Figure 18. Calibration and validation of different land covers for the years (a) 2013, (b) 2015, and (c) 2018

data, while the yellow line shows the model's best simulation output. The time series is divided into two main segments: calibration (left of the vertical dashed line) and validation (right of the vertical dashed line). Calibration involves adjusting model parameters to fit observed data, while validation tests the model's performance on separate data to evaluate its predictive capability.

Across all three LULC scenarios, the model demonstrates a reasonable fit to the observed discharge data, with the best simulation line closely following the observed discharge line for both calibration and validation periods. It suggests that the model calibration process was successful for each LULC year, showcasing the ability of the model to simulate stream flow under different land cover conditions. The observed data generally falls within the uncertainty range, indicating that the model captures the variability in stream flow reasonably well. However, some observed peaks and valleys fall outside the uncertainty bounds, suggesting periods of less accurate simulation during high or low flow conditions. Comparing the three LULC years, there is consistency in model performance, though slight differences may reflect the impact of land cover changes on stream flow.

On the other hand, Table 7 shows the statistical measures used to evaluate the accuracy of the calibrated and validated values, including R^2, NSI, and PBIAS. The values obtained for these measures were promising, indicating that the calibrated and validated values were accurate and reliable. Overall, the study suggests that the calibrated and validated values for land use in 2021 were reliable and consistent with the historical trends. It was important for making informed decisions about land use and resource management (Santhi et al., 2001).

Table 8
Values of parameters for different land covers for the years 2013, 2015 and 2018

YEARS	Calibration			Validation		
	R^2	NSI	PBIAS	R^2	NSI	PBIAS
2013	0.63	0.21	−32.1	0.88	0.76	−19
2015	0.63	0.20	−32.1	0.87	0.76	−16.4
2018	0.63	0.20	−32.1	0.89	0.78	−17

CONCLUSION

The study conducted within the Taguibo River Watershed Forest Reserve (TRWFR) in Butuan City, Philippines, highlights the role of hydrological modeling in effectively managing water resources amidst the challenges posed by rapid urban development and climate change and utilizing the Geographic Information System (GIS) and the Soil and Water Assessment Tool (SWAT), the researchers successfully calibrated and validated a hydrological model that demonstrated a strong correlation between simulated and observed discharge data, affirming its effectiveness in simulating watershed hydrology. Key findings

Aljon Ente Bocobo, Arnold Gemida Apdohan, Antonietto Ortega Cacayan Jr., Kenneth John Peña Lajera and
Febe Hyacinth Andoy Simbolas

from the study revealed that the watershed, characterized by a predominance of forest land and steep slopes, exhibits significant annual variability in water yield, influenced by precipitation patterns and land use changes. The outputs of the model provide valuable insights into the dynamics of water yield across the sub-basins. The research emphasizes the necessity of integrating advanced modeling tools like SWAT and GIS in water resource assessments, particularly in areas facing environmental pressures. By addressing the interplay between land cover, hydrology, and climate factors, this study contributes to a deeper understanding of watershed dynamics. It offers a foundation for informed decision-making in water resource management and conservation efforts in the Taguibo River Watershed Forest Reserve. The findings encourage continued research and collaboration among stakeholders to enhance water supply management and mitigate the impacts of climate change, ensuring the sustainability of water resources in the future.ng population.

ACKNOWLEDGEMENT

REFERENCES

Abbaspour, K. C., Rouholahnejad, E., Vaghefi, S., Sirinivasan, R., Yang, H., & Klove, B. (2015). A continental-scale hydrology and water quality model for Europe: Calibration and uncertainty of a high-resolution large-scale SWAT model. *Journal of Hydrology*, *524,* 733–752. https://doi.org/10.1016/j.jhydrol.2015.03.027

Arnold, J. G., Moriasi, D. N., Gassman, P. W., Abbaspour, K. C., & White, M. J. (2012). SWAT: Model use, calibration, and validation. *Transactions of the ASABE*, *55*(4), 1491-1508.

Arnold, J. G., Srinivasan, R., Muttiah, R. S., & Williams, J. R. (1998). Large area hydrologic modeling and assessment part I: Model development. *Journal of the American Water Resource Association*, *34*(1), 73-89. https://doi.org/10.1111/j.1752-1688.1998.tb05961.x

Ayivi, F., & Jha, M. K. (2018). Estimation of water balance and water yield in the reedy fork-buffalo creek watershed in North Carolina using SWAT. *International Soil and Water Conservation Research, 6*(3), 203-213. https://doi.org/10.1016/j.iswcr.2018.03.007

Bracmort, K. S., Arabi, M., Frankenberger, J. R., Engel, B. A., & Arnold, J. G. (2006). Modelling long-term water quality impact of structural BMPs. *Transactions of the ASABE, 49*(2), 367-374.

Farzana, S. Z., Zafor, M. A., & Shahariar, J. A. (2019). Application of SWAT model for assessing water availability in Surma River Basin. *Journal of the Civil Engineering Forum, 5*(1), 29-38. https://doi.org/10.22146/jcef.39191

Galintao, R. O., & Santillan, M. M. (2020, November 16-19). Using remote sensing and GIS to identify alternative water sources for Butuan City, Philippines. [Paper presentation]. IEEE Region 10 Conference (TENCON), Osaka, Japan. https://doi.org/10.1109/TENCON50793.2020.9293724

Guo, Q., Yu, C., Xu, Y., Yang, Y., & Wang, X. (2023). Impacts of climate and land-use changes on water yields: Similarities and differences among typical watersheds distributed throughout China. *Journal of Hydrology: Regional Studies*, *45,* Article 101294. https://doi.org/10.1016/j.ejrh.2022.101294

Gupta, H. V., Sorooshian, S., & Yapo, P. O. (1999). Status of automatic calibration for hydrologic models: Comparison with multilevel expert calibration. *Journal of Hydrologic Engineering, 4*(2), 135-143. https://doi.org/10.1061/(ASCE)1084-0699(1999)4:2(135)

Khoury, I. A., Boithias, L., & Labat, D. (2023). A review of the application of the soil and water assessment tool (SWAT) in karst watersheds. *Water, 15*(5), Article 954. https://doi.org/10.3390/w15050954.

Kodoatie, R. J., & Sjarief, R. (2010). *Tata ruang air*. Penerbit Andi.

Koltsida, E., Mamassis, N., & Kallioras, A. (2023). Hydrological modeling using the soil and water assessment tool in urban and peri-urban environments: The case of Kifisos experimental subbasin (Athens, Greece). *Hydrology and Eart Science System, 27*(4), 917–931. https://doi.org/10.5194/hess-27-917-2023

Li, X., Sun, W., Zhang, D., Huang, J., Li, D., Ding, N., Zhu, J., Xie, Y., & Wang, X. (2021). Evaluating water provision service at the sub-watershed scale by combining supply, demand, and spatial flow. *Ecological Indicators, 127,* Article 107745. https://doi.org/10.1016/j.ecolind.2021.107745

Moriarty, P., Batchelor, C., & Laban, P. (2005). *Using water resources assessments within the empower planning cycle for IWRM* (Working Paper No. 4). Empowers Partnership. https://www.researchgate.net/publication/265432676_Using_Visions_Scenarios_and_Strategies_within_the_EMPOWERS_Planning_Cycle_for_IWRM

Oda, T., Iwasaki, K., Egusa, T., Kubota, T., Iwagami, S., Iida, S. I., Momiyama, H., & Shimizu, T. (2024). Scale-dependent inter-catchment groundwater flow in forested catchments: Analysis of multi-catchment water balance observations in Japan. *Water Resources Research, 60*(7), Article e2024WR037161. https://doi.org/10.1029/2024WR037161

Refsgaard, J. C., & Storm, B. (1996). Construction, calibration, and validation of hydrological models. In M. B. Abbott & J. C. Refsgaard (Eds.) *Distributed Hydrologic Modeling* (pp. 41–54). Springer. https://doi.org/10.1007/978-94-009-0257-2_3

Saleh, A., Arnold, J. G., Gassman, P. W. A., Hauck, L. M., Rosenthal, W. D., Williams, J. R., & McFarland, A. M. S. (2000). Application of SWAT for the upper North Bosque River watershed. *Transactions of the ASAE, 43*(5), 1077-1087.

Sanguila, M. B., Cobb, K. A., Siler, C. D., Diesmos, A. C., Alcala, A. C., & Brown, R. M. (2016). The amphibians and reptiles of Mindanao Island, southern Philippines, II: The herpetofauna of northeast Mindanao and adjacent islands. *ZooKeys*, *624*, Article 1–132. https://doi.org/10.3897/zookeys.624.9814

Santhi, C., Arnold, J. G., Williams, J. R., Dugas, W. A., Srinivasan, R., & Hauck, L. M. (2001). Validation of the SWAT model on a large river basin with point and nonpoint sources. *JAWRA Journal of the American Water Resources Association, 37(5), 1169-1188*. https://doi.org/10.1111/j.1752-1688.2001.tb03630.x

Santillan, J., Makinano, M., & Paringit, E. (2011). Integrated Landsat image analysis and hydrologic modeling to detect impacts of 25-year land-cover change on surface runoff in a Philippine watershed. *Remote Sensing, 3*(6), 1067-1087. https://doi.org/10.3390/rs3061067

Shivhare, N., Rahul, A. K., Omar, P. J., Chauhan, M. S., Gaur, S., Dikshit, P. K. S., & Dwivedi, S. B. (2018). Identification of critical soil erosion prone areas and prioritization of micro-watersheds using geoinformatics techniques. *Ecological engineering, 121*, 26-34. https://doi.org/10.1016/j.ecoleng.2017.09.004

Young, G. J., Dooge, J. I., & Rodda, J. C. (1994). *Global water resource issues*. Cambridge University Press.